AAAS
Journal of Remote Sensing
Volume 2022, Article ID 9769536, 14 pages
https://doi.org/10.34133/2022/9769536

Journal of Remote Sensing
A SCIENCE PARTNER JOURNAL

Review Article

An Introduction to the Chinese High-Resolution Earth Observation System: Gaofen-1~7 Civilian Satellites

Liangfu Chen,[1,2] Husi Letu,[1] Meng Fan,[1] Huazhe Shang,[1] Jinhua Tao,[1] Laixiong Wu,[1] Ying Zhang,[1] Chao Yu,[1] Jianbin Gu,[1] Ning Zhang,[3] Jin Hong,[4] Zhongting Wang,[5] and Tianyu Zhang[1]

[1]*State Key Laboratory of Remote Sensing Science, The Aerospace Information Research Institute, Chinese Academy of Sciences (CAS), Datun Road No. 20 (North), Beijing 100101, China*
[2]*University of Chinese Academy of Sciences (UCAS), Beijing 100101, China*
[3]*Remote Sensing Application Center, Ministry of Housing and Urban-Rural Development of the People's Republic of China, Sanlihe Road No. 9 Beijing 100835, China*
[4]*Key Laboratory of Optical Calibration and Characterization of Chinese Academy of Science, Anhui Institute of Optics and Fine Mechanics, Chinese Academy of Sciences, Hefei 230031, China*
[5]*Center for Satellite Application on Ecology and Environment, Ministry of Ecology and Environment, Beijing 100006, China*

Correspondence should be addressed to Husi Letu; husiletuw@hotmail.com and Jinhua Tao; taojh@irsa.ac.cn

Received 9 June 2021; Accepted 7 March 2022; Published 8 April 2022

The Chinese High-resolution Earth Observation System (CHEOS) program has successfully launched 7 civilian satellites since 2010. These satellites are named by Gaofen (meaning high resolution in Chinese, hereafter noted as GF). To combine the advantages of high temporal and comparably high spatial resolution, diverse sensors are deployed to each satellite. GF-1 and GF-6 carry both high-resolution cameras (2 m resolution panchromatic and 8 m resolution multispectral camera), providing high spatial imaging for land use monitoring; GF-3 is equipped with a C-band multipolarization synthetic aperture radar with a spatial resolution of up to 1 meter, mostly monitoring marine targets; GF-5 carried 6 sensors including hyperspectral camera and directional polarization camera, dedicated to environmental remote sensing and climate research, such as aerosol, clouds, and greenhouse gas monitoring; and GF-7 laser altimeter system payload enables a three-dimensional surveying and mapping of natural resource and land surveying, facilitating the accumulation of basic geographic information. This study provides an overview of GF civilian series satellites, especially their missions, sensors, and applications.

1. Introduction

The China High-resolution Earth Observation System (CHEOS) was first proposed in 2006, which was officially stimulated into substantial operation as one of the Chinese National Science and Technology Major Projects in May 2010. China National Space Administration (CNSA) and Earth Observation System and Data Center of CNSA (EOSDC-CNSA) are responsible for constructing and organizing the CHEOS, respectively [1, 2]. The CHEOS forms an integrated system including three main parts (i.e., space-based, ground, and application systems). The CHEOS with the characteristic of high spatial, temporal, and spectral resolution is aimed at newly establishing an all-day, all-weather coverage Earth observation system for satisfying the requirements of social development.

Gaofen (meaning high resolution in Chinese, hereafter noted as GF) series are the space-based part of the whole CHEOS project. The GF satellites have multiobservational capabilities of high spatial, spectral, and temporal resolution and high precision, including laser altimeters and passive sensors measuring visible light, infrared, and microwave spectrum at multiple bands or hyperspectral resolution. Currently, the CHEOS project has successfully launched three multispectral satellites with high spatial resolution (GF-1, GF-2, and GF-6), one high-resolution radar satellite (GF-3), one optical geostationary satellite (GF-4), one high spectral and atmospheric observation satellite (GF-5), and one

Table 1: Introduction of GF-1 to GF-7 satellites, all satellites except GF-4 (geosynchronous) are solar synchronous.

Gaofen series		Launch time	Sensor	Main service tasks
Panchromatic multispectral camera	GF-1	2013.04.26	2 panchromatic multispectral cameras (2 m panchromatic, 8 m); 4 multispectral wide-width cameras (16 m)	Land resources and agricultural meteorology
	GF-2	2014.08.19	2 panchromatic multispectral cameras (panchromatic 1 m, substar point 0.8 m, multispectral 4 m)	Land and resources, urban management, transportation
	GF-6	2018.06.02	1 panchromatic multispectral camera (2 m panchromatic, 8 m); 1 multispectral wide-width camera (16 m)	Land resources, agricultural meteorology, identification of ground crops
Multipolar synthetic aperture radar	GF-3	2016.08.01	C-band multipolarization synthetic aperture radar (1~500 m)	Marine application, disaster processing, water protection and management, meteorology prevention, mitigation of emergent disasters
Environmental satellite	GF-5	2018.05.09	AHSI, VIMS, AIUS, EMI, GMI, DPC	Monitoring atmospheric aerosol, sulfur dioxide, nitrogen dioxide, methane, water quality, straw burning, urban heat island
All-sky staring camera and radar altimeter	GF-4	2015.12.29	Staring camera with visible (50 m) and near infrared (400 m)	Remote sensing of disaster reduction, forestry, meteorology
	GF-7	2019.11.03	A dual-linear array camera (back sight: 0.65 m, fore sight: 0.8 m); multispectral (back sight: 2.6 m); a laser altimeter (ranging accuracy ≤ 0.3 m) (slope is less than 15 degrees); a footprint camera (≤4 m)	Agricultural surveying and mapping of topography

three-dimensional mapping satellite (GF-7). All the above satellites had been launched and put into service before 2020. Data products of the GF satellite series have successfully and effectively supported applications in the field of land-use planning, environmental monitoring of ecology, atmosphere, and water, etc. CHEOS promotes the transformation and upgrading of satellite systems from "focusing on research and test" to "the balance between test and operation," formulates the satellite product and application system with Chinese flavors, and progressively provides global services.

This review presents the Chinese High-resolution Earth Observation System and the Gaofen satellites with a focus on their orbit and sensor configurations, data products, and relevant applications. Section 2 introduces the mission satellite platforms, sensors, and their ways of observation. Section 3 describes typical data products and their applications in environmental protection, terrain, and agriculture monitoring. Section 4 discusses the current usage of GF series satellites and plans about its future extension or improvement.

2. Mission Payloads

The scientific payloads aboard GF-1~7 civilian satellites have been demonstrated to cover different ways of observations, from radar and panchromatic cameras to polarization and hyperspectral imagers. The orbital setting includes both solar synchronous and geosynchronous. This section will elaborate on the sensors and their specific bands and observation configurations. Because of similarities between GF-1/2 and GF-6, these three satellites are grouped together.

2.1. Sensors of GF-1~GF-7 Satellites and Their Observation Targets. The launch time and main sensors for GF-1~7 are listed, respectively, in Table 1. On April 26, 2013, the GF-1 satellite was launched and carried two panchromatic cameras and four multispectral broadband cameras with 16-meter resolution. The GF-1 satellite products include two categories: PMS and WFV. The data of PMS include level 1 and level 2 image products. The WFV Raster Type supports level 1A and level 1C standard products distributed by the Resource Satellite Application Center and has a variety of built-in processing templates to simplify data use and management. Users can log in to the resource satellite data distribution platform in the center of the query and order (http://36.112.130.153:7777/DSSPlatform/index.html). The GF-1 satellite is mainly used in public security, disaster protection, drift monitoring, urban land investigation, and other fields. The wide range of observation data of GF-1 mainly serves the needs of land resource management and agricultural meteorology industries. The multispectral sensor loaded in GF-1 consists of two types of cameras, namely, the high-resolution camera (PMS) and wide-field camera (WFV). On August 19, 2014, the GF-2 satellite was launched and carried two panchromatic and multispectral cameras with 1-meter and 4-meter resolution, respectively. The spatial resolution of the subsatellite points reached 0.8 meters. The GF-2 satellite data provides level 1 relative radiometric correction products and PMS (0.8 m panchromatic and 3.2 m

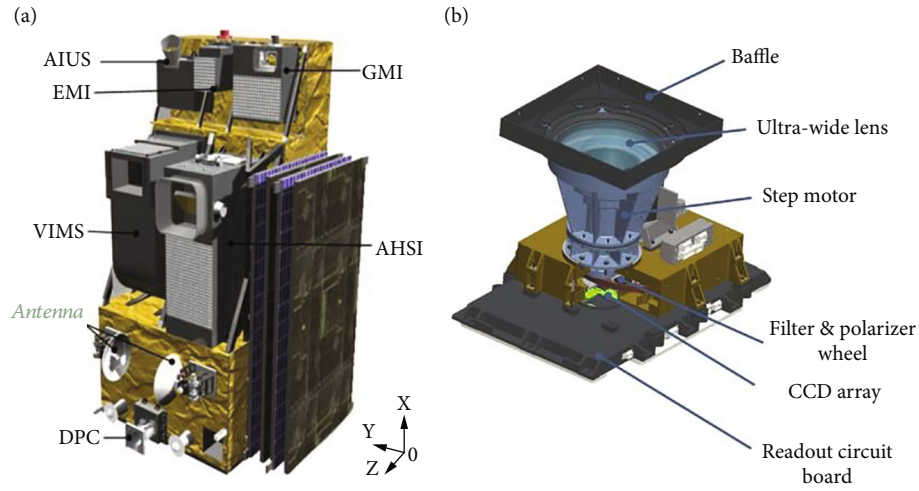

Figure 1: Instrumental parameters of the GF-5 satellite (a) and the DPC sensor (b).

Table 2: The orbit specification of GF-1 and GF-2.

Information	GF-1	GF-2
Rail type	Sun synchronous regression orbit	Sun synchronous regression orbit
Orbital altitude (km)	645	631
Orbit inclination (°)	98.05	97.90
Local time (descending)	10:30 AM	10:30 AM
Side swing ability (rolling)	±25°, motor time of 25° ≤ 200 s, ability of emergency side swing (roll) ± 35°	±35°, the motor time of 35° ≤ 180 s

Table 3: The sensor configurations for GF-1 and GF-2.

Parameter		GF-1		GF-2
		Panchromatic (PAN)/multispectral camera (MS)	Multispectral camera (MS)	Panchromatic (PAN)/multispectral camera (MS)
Spectral range (μm)	PAN	0.45–0.90		0.45–0.90
	B1/blue	0.45–0.52	0.45–0.52	0.45–0.52
	B2/green	0.52–0.59	0.52–0.59	0.52–0.59
	B3/red	0.63–0.69	0.63–0.69	0.63–0.69
	B4/NIR	0.77–0.89	0.77–0.89	0.77–0.89
Spatial resolution (m)	PAN	2 m	16 m	1 m
	MS	8 m		4 m
Swath width (km)		60 (2 cameras)	800 (4 cameras)	45
Revisit cycle (side-sway)/day		4		5
Covering the period (no side swing)/day		41	4	69

multispectral) data products. The resolution of the sensor carried by the GF-2 satellite is higher than that of the GF-1 satellite, which resolution reaches panchromatic 1 m/multispectral 4 m, and the camera realizes the function of amplitude mapping. The GF-2 satellite provides demonstration application services for high-precision land use survey. On August 10, 2016, the GF-3 satellite was launched and carried a C-band, multipolarized synthetic aperture radar, which can operate at all weather conditions regardless of day or night and can penetrate through clouds, surface vegetation, loose sand layer, and ice and snow. The GF-3 satellite ground system produces level 1-2 standard products. The GF-3 satellite is widely used in marine right protection, disaster risk warning and forecast, water resource management, and weather forecasting. The GF-3 satellite is China's first C-band multipolarization synthetic aperture radar (SAR) satellite with a resolution of 1 m, which has 12 imaging modes. The GF-4 satellite was launched on December 29, 2015, carrying an area scan camera that measures visible light nadir at 50 m resolution and medium-wave infrared nadir at 400 m resolution. The GF-4 satellite has a high resolution of 50 m visible light/400 m midwave infrared. GF-4 data application includes disaster monitoring,

Table 4: Sensor configurations for GF-3.

Name of imaging mode		Resolution (m)	Width (km)	Polarization mode
Spotlight mode (SL)		1	10	Single polarization
Strip model	Hyperfine strip (UFS)	3	30	Single polarization
	Fine strip 1 (FSI)	5	50	Double polarization
	Fine strip 2 (FSII)	10	100	Double polarization
	Standard strip model (SS)	25	130	Double polarization
	Quad polarization strip I (QPSI)	8	30	Full polarization
	Quad polarization strip II (QPSII)	25	40	Full polarization
Scan model	Narrow scan mode (NSC)	50	300	Double polarization
	Wide scan mode (WSC)	100	500	Double polarization
	Global observation model (GLO)	500	650	Double polarization
Wave imaging model (WAV)		10	5	Full polarization
Extended incident angle model (EXT)	Low angle of incidence	25	130	Double polarization
	High angle of incidence	25	80	Double polarization

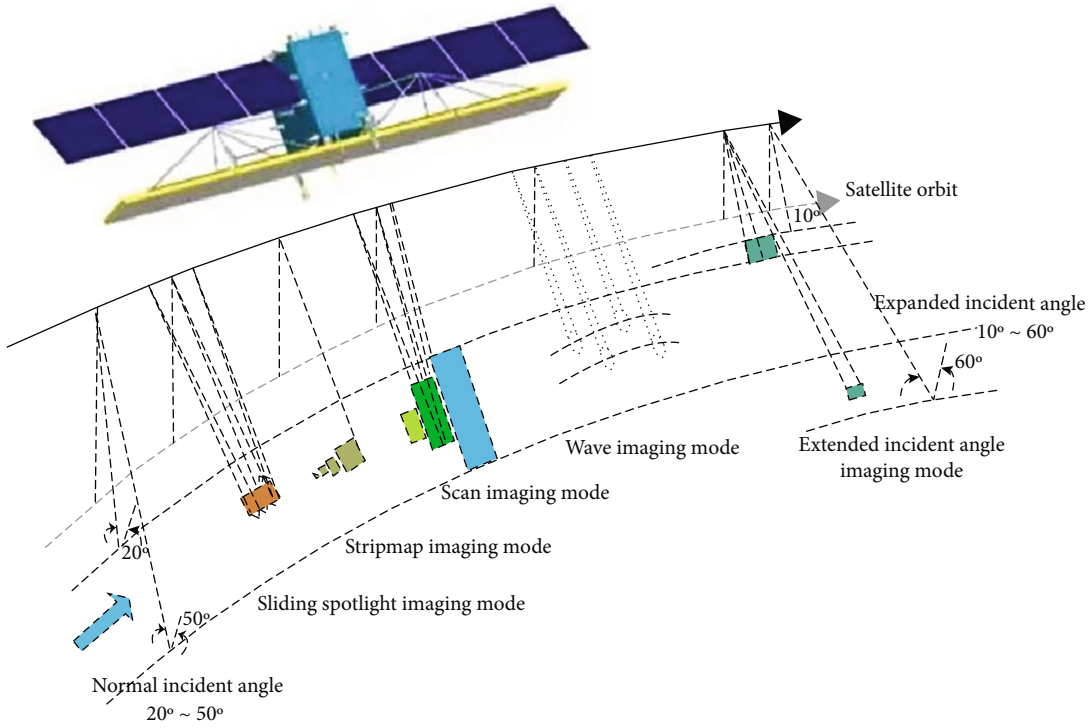

Figure 2: Different working modes of C-SAR onboard GF-3 [11].

meteorological observation agriculture, and national security. It enables an advanced technology for alerting natural disasters and monitoring wildfires or typhoons [3].

The GF-5 satellite, as the first satellite mission in China specifically for air quality monitoring, was launched at the date of May 9, 2018. Six sensors onboard GF-5 include a directional polarization camera (DPC) for aerosol and cloud (Figure 1). The GF-5 satellite data product system contains 4- to 6-level application products. The Environmental Trace Gases Monitoring Instrument (EMI) is aimed at monitoring atmospheric trace gases for understanding global atmospheric information [4], which is similar to the Ozone Monitoring Instrument (OMI) [5, 6]. The main objective of the Greenhouse Gas Monitoring Instrument (GMI) payload is studying the source and sink of tropospheric greenhouse gases (e.g., CO_2 and CH_4) [7], through using a spatial heterodyne spectroscopy (SHS) interferometer to acquire interferograms. The Atmospheric Infrared Ultraspectral Sounder (AIUS), as the Chinese first official occultation spectrometer, is a Fourier transform infrared spectrometer for measuring O_3 and other species in the stratosphere and upper troposphere over the Antarctic [8], a visible/short-wave infrared

Table 5: Information of the sensors on GF-4.

Information	Panchromatic and near-infrared sensor	Intermediate infrared sensor
Spectral range	B1: 450~900 nm B2: 450~520 nm B3: 520~600 nm B4: 630~690 nm B5: 760~900 nm	B6: 3.5 μm~4.1 μm
Focal length	6600 mm	1350 mm
Pixel size	9 μm	15 μm
Planar array sensor	10240 × 10240 CMOS	1024 × 1024 HgCdTe detector
Ground sample distance	50 m	400 m
Region of imaging	500 km × 500 km	400 km × 400 km
Field angle	0.8° × 0.8°	0.66° × 0.66°
Time of integration	0.5 ms~100 ms	0.1 ms~10 ms

hyperspectral spectrometer, and a spectral imager. Except for using atmospheric parameters, the GF-5 satellite can also be used for monitoring other environmental factors.

The GF-6 satellite was launched on June 2, 2018. It carries a panchromatic imager at 2 m resolution, multispectral high-resolution camera at 8-meter resolution, and a multispectral medium resolution wide-band camera at 16-meter resolution similar to GF-1. It obtains a wide range of Earth observation data through networking with the GF-1 satellite. The GF-6 satellite data product system includes level 1 and 2 standard data products, level 3 basic products, level 4 and 5 generic products, and level 6 thematic products (agriculture, forestry, and disaster reduction). The GF-7 satellite launched on November 3, 2019, carries the first spaceborne laser altimeter system developed in China [9, 10]. The two-line array stereoscopic camera carried by GF-7 can effectively acquire panchromatic stereoscopic images with a width of 20 km and a resolution of better than 0.8 m and multispectral images with a resolution of 3.2 m. Through the composite mapping mode of stereoscopic camera and laser altimeter, 1 : 10,000 scale stereoscopic mapping can be achieved. Currently, available data of GF series satellites mainly include GF-1 to GF-7. High-resolution satellite data can be found on the websites. The GF-1~GF-7 satellite has 39 common products, including two geometric products, namely, orthophoto product DOM and terrain product DSM. There are 6 kinds of radiation basic products, including surface reflectance, water-free emissivity, radar backscattering coefficient, cloud mask, atmospheric aerosol optical thickness, and atmospheric water vapor content. Two types of land cover products are land cover type and land use type, respectively. Nine kinds of energy balance products include surface albedo, surface emissivity, land surface temperature, sea surface temperature, soil heat flux, photosynthetically active radiation, downward shortwave radiation, longwave radiation, and net radiation products. There are 10 kinds of vegetation parameter products, including vegetation index, leaf area index, vegetation coverage, photosynthetically active radiation absorption ratio, net primary productivity, vegetation phenology, canopy chlorophyll content, chlorophyll fluorescence, forest biomass, and tree height.

Table 6: Information of the AHSI [12].

Characteristic	On-orbit calibration
Spectral range (μm)	0.39~2.513
Spectral resolution (nm)	4.31 (VNIR); 7.96 (SWIR)
Ground sampling distance (m)	30
Swath width (km)	59.75
X-track spectral error (nm)	0.23 (VNIR); 0.20 (SWIR)
MTF	~0.3
SNR	686 (600 nm); 369 (900 nm) 452 (1200 nm); 460 (1500 nm) 405 (1700 nm); 194 (2400 nm)

Table 7: Information of the VIMS.

Spectral range	VNIR	Band 1: 0.45–0.52 μm Band 2: 0.52–0.6 μm Band 3: 0.62–0.68 μm Band 4: 0.76–0.86 μm
	SWIR	Band 5: 1.55–1.75 μm Band 6: 2.08–2.35 μm
	MIR	Band 7: 3.5–3.9 μm Band 8: 4.85–5.05 μm
	TIR	Band 9: 8.01–8.39 μm Band 10: 8.42–8.83 μm Band 11: 10.3–11.3 μm Band 12: 11.4–12.5 μm
Spatial resolution	VNIR/SWIR MIR/TIR	20 m 40 m
Swath width		60 km

There are 10 kinds of water yield products, including soil moisture content, evapotranspiration, drought index, surface water, glacier cover, snow cover, snow cover index, water suspended matter concentration, water chlorophyll concentration, and water transparency. The specific information can be accessed on the comprehensive service information sharing platform (http://gaofenplatform.com/channels/61.html).

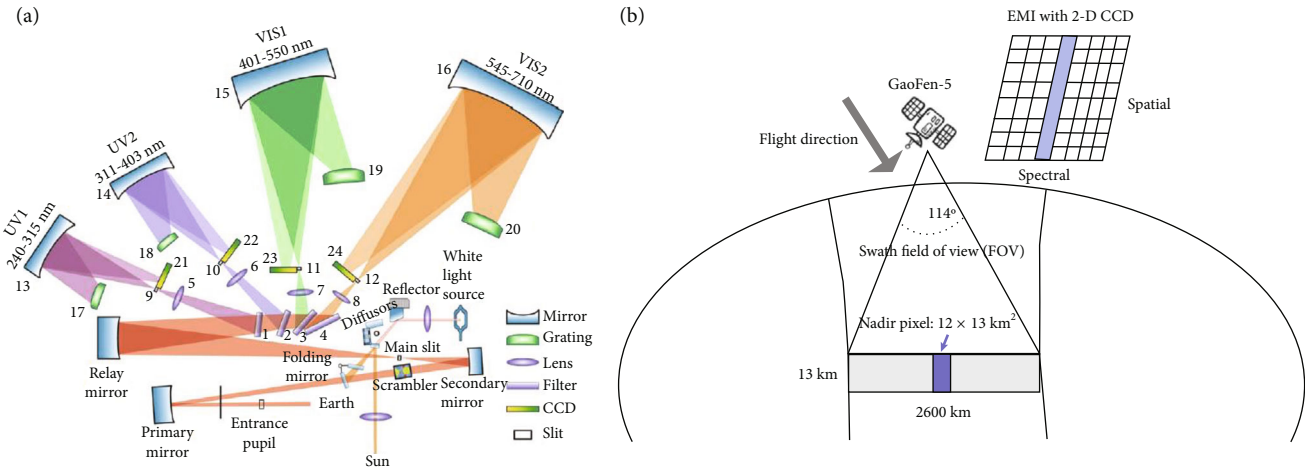

Figure 3: Illustration of the operating principle of the EMI [6].

2.2. Introduction of Sensors on GF-1/2/6. The GF-1 satellite obtains multispectral and high spatial-temporal resolution imaging of the ground by cooperation with two panchromatic, multispectral cameras and four multispectral cameras with a resolution of 2 m, 8 m, and 16 m resolution, respectively. It also improves the swath width of satellite images. The imaging information from these sensors can directly provide users with joint high-definition images through image fusion technology and stable attitude control technology of satellite platforms. The lifetime of GF-1 is 5 to 8 years. The GF-2 satellite further improves its spatial resolution based on GF-1 and carried two high-resolution cameras (1 m resolution panchromatic and 4 m resolution multispectral camera) (Table 2). GF-2 has the ability to obtain submeter spatial resolution satellite observations. The GF-6 satellite is China's first engineering remote sensing satellite which is efficient in combining high-resolution and wide coverage imaging capability. With a high-resolution camera (2 m panchromatic, 8 m multispectral) and a wide spectrum camera (16 m multispectral), the addition of GF-6 further enriches the application of this kind of data in precision agriculture. GF-6 satellite and GF-1 satellite basically have the same resolution setting that the new purple band, yellow band, red band 1, and red band 2 are added to the spectrum (Table 3). The swath width of the image from GF-6 width is larger than that of the GF-1 satellite, reaching 1000 km.

2.3. GF-3 Synthetic Aperture Radar (SAR) Imaging. The GF-3 satellite is the first C-band multipolarization synthetic aperture radar (C-SAR) imaging satellite in China with one-meter resolution. It is an important basis for the high-resolution series project to achieve the objective of time-space coordination and all-weather and all-sky Earth observation. The satellite has up to 12 imaging modes, making it one of the SAR satellites with the most imaging modes in the world (Table 4). Figure 2 shows the different working modes of C-SAR onboard GF-3. Combined with the advantages of high spatial resolution, satellite imaging can realize not only large-scale census but also detailed survey of specific areas, which can meet the needs of different users for different targets of imaging.

Table 8: Information of the EMI.

Spectral range	UV1: 240-315 nm UV2: 311-403 nm VIS1: 401-550 nm VIS2: 545-710 nm
Spectral sampling	UV1: 0.08 nm; UV2: 0.09 nm VIS1: 0.12 nm; VIS2: 0.13 nm
Spectral resolution	0.3-0.5 nm
Telescope swath IFOV	114° (2600 km on the ground)
Telescope flight IFOV	0 (6.5 km on the ground)
Charge coupled device (CCD) detectors	UV: 1072 × 1032 (spectral × spatial) pixels VIS: 1286 × 576 (spectral × spatial) pixels 13 km × 48 km (electronic binning factor)
Ground pixel size at the nadir	UV: 24, VIS: 16 13 km × 8 km (UV, binning factor 4) 13 km × 12 km (VIS, binning factor 4)

The image resolution and width have a good balance of 1-500 m and 10-650 km, respectively. The noise equivalent backscattering coefficient is better than -19 dB in a 1-10 m image resolution and better than -21 dB in 25-500 m. The satellite is designed to have an in-orbit life of 8 years, and its absolute radiometric accuracy reaches 1.5 dB (one scene) and 2 dB (long term). The satellite's attitude control can realize continuous 2d attitude movement because of high precision and stability [12].

2.4. Introduction of Sensors on GF-4. The geostationary satellite GF-4 orbits the Earth at a height of about 36,000 km, and it can perform fixed-point continuous observations with a stationary position of 105.6°E. The temporal resolution reaches up to 20 s. The spatial resolution is 50 m for visible and near-infrared bands and 400 m for medium-wave infrared bands. GF-4 can provide four observation modes, including census, gazing monitoring, area monitoring, and

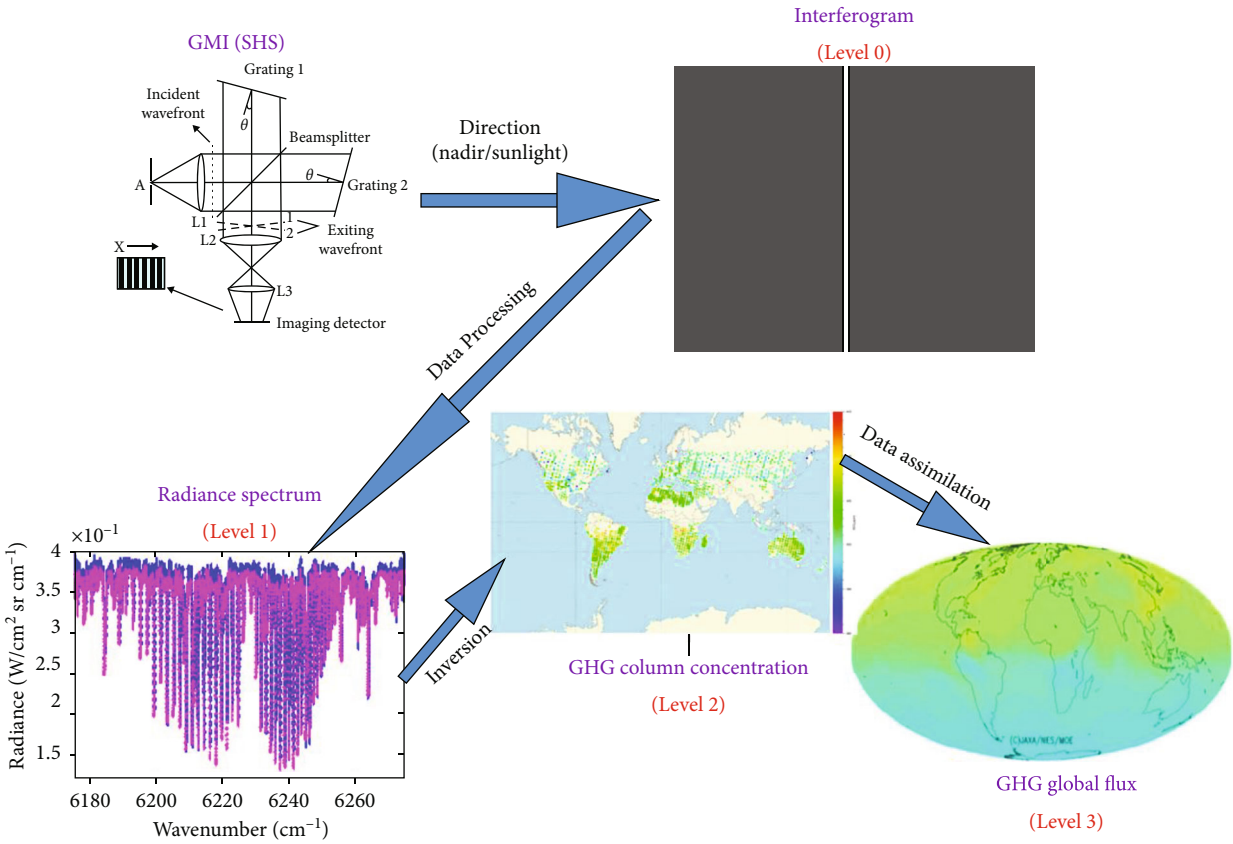

Figure 4: Illustration of the operating principle of the GMI [7].

motorized inspection modes. GF-4 is equipped with an optical camera and three star trackers. A panchromatic near-infrared sensor and an intermediate infrared sensor are installed in an optical camera. They use the same set of optical lenses and use a color separation filter to distinguish signals in different bands (Table 5).

2.5. Introduction of 6 Sensors on GF-5. The GF-5 is designed for a sun-synchronous orbit (orbital inclination 98.218°). It orbits the Earth every 98.805 minutes, thus making 14.57 trips per day, with the ascending node at 1:30 PM. GF-5 is China's first high-resolution satellite for atmospheric pollution. Its 6 sensors include the hyperspectral imaging satellite developed by China. We introduced the six sensors orderly as follows.

(1) *AHSI*: AHSI is a VIS and SWIR hyperspectral sensor, which is also the first space-based hyperspectral spectrometer of China with convex grating spectrophotometry and an improved three concentric-mirror (Offner) configuration [13]. The spectrum of AHSI ranges from 400 to 2500 nm with the spectral resolution of 5-10 nm and the band number of 330 (Table 6).

(2) *VIMS*: with the high spatial resolution, the VIMS can be used for environment monitoring, urban heat island, water management, geological survey, and natural disasters [14]. The swath width is 60 km, and the spectrum of 12 bands covers the range of 0.45 to 12.5 μm. The spatial resolution is 20 m for visible, near-infrared, and shortwave images and 40 m for middle infrared (MIR) and thermal infrared (TIR) images. The four TIR bands of VIMS are centered at 8.20 (8.01~8.39 μm), 8.63 (8.42~8.83 μm), 10.80 (10.30~11.30 μm), and 11.95 μm (11.40~12.50 μm), respectively (Table 7).

(3) *EMI*: the EMI can be used for monitoring pollutant gas columns by measuring the unique and narrow absorption structures of different trace gases in the ultraviolet (UV) and VIS spectral region [6]. The spatial resolution in the nadir direction reaches $12 \times 13\,km^2$ (Figure 3, Table 8). The detecting spectrum of EMI covers 2 UV bands and 2 VIS bands.

(4) *GMI*: two observation modes, nadir and sun glint, are involved into the GMI (Figure 4). It records the solar light including one NIR band (oxygen band, 0.76 μm) and three SWIR bands (1.58, 1.65, and 2.0 μm) (Table 9). 1.58 and 1.65 μm bands are weak

Table 9: Information of the GMI [7].

Specifications	Values			
	Band 1	Band 2	Band 3	Band 4
Detected gas	O_2	CO_2	CH_4	CO_2
Band range (μm)	0.759-0.769	1.568-1.583	1.642-1.658	2.043-2.058
Spectral resolution (cm^{-1})	0.6		0.27	
SNR (albedo = 0.3 ; sun elevation = 30°)	300		250	
Radiometric calibration	Absolute accuracy: 5%, relative accuracy: 2%			
FOV	14.6 mrad (10.3 km@705 km)			
Scan	Cross-track (±35 deg), along track (±20 deg)			
Observation modes	Nadir: 1, 5, 7, 9 points (default mode is 5 points); sun glint; calibration			
Number of detector pixels	1024 × 1024	512 × 640	512 × 640	256 × 320
Zero optical path difference pixel	512	235	235	75
Sampling form	Symmetric	Asymmetric	Asymmetric	Asymmetric

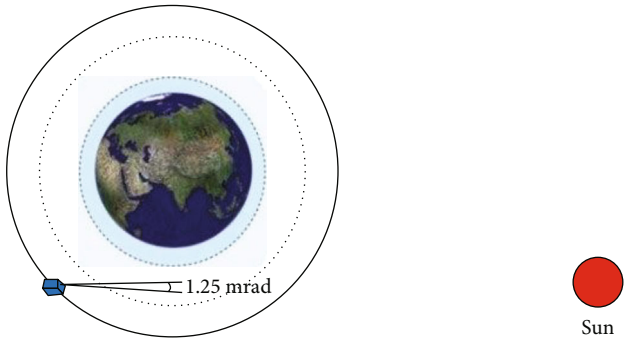

Figure 5: AIUS measurement geometry [8].

Table 10: Information of the AIUS [8].

Parameters	AIUS
Observation mode	Solar occultation
Spectral range	750-4100 cm^{-1}
Spectral resolution	0.03 cm
Field of view (FOV)	1.25 mrad
Signal-to-noise ratio (SNR)	1000-2000 cm^{-1} : 200-350 2000-3200 cm^{-1} : >300 Other spectral bands: 100-200

absorption bands of CO_2 and CH_4 which is highly sensitive to the near-surface CO_2 and CH_4 concentrations. As a strong absorption band of CO_2, 2.0 μm band contains additional CO_2 information. And the NIR oxygen band can provide the surface pressure and cloud and aerosol parameters for CO_2 and CH_4 retrieval.

(5) *AIUS*: the AIUS instrument is a spaceborne Michelson interferometer for measuring occultation transmittance spectra in the middle and upper atmosphere (Figure 5). AIUS measures atmospheric limb emission spectra from 750 cm^{-1} to 4100 cm^{-1}, with a spectral resolution of 0.03 cm^{-1} (Table 10). It is composed of MCT (mercury cadmium telluride, 750–1850 cm^{-1}) and InSb (1850–4160 cm^{-1}) bands. The instrument ranges from 8 to 100 km above sea level with a field of view (FOV) of 1.25 mrad.

(6) DPC is able to take the measurements from up to 11 viewing angles per pixel, while the number of valid observations relies on the relative relation between solar zenith angle and satellite zenith angle. In total, there are 8 wavelengths, and 3 of them (490, 670, and 865 nm) provide both total and polarized radiance. The 763 and 765 nm channel enables cloud top pressure retrieval, and the 910 nm channel enables water vapor retrieval. The DPC is equipped with a charge coupled device (CCD) with effective pixels (512 × 512) from the useful pixels (544 × 512), realizing 3.3 km spatial resolution under a swath width of 1850 km. The 2-day revisit period allows it effectively observing the tendency of atmospheric pollution. The DPC specifications are listed in Table 11.

2.6. The Working Principle and Parameters of GF-7. The GF-7 satellite is a laser altimeter system with the angle between each beam and the nadir of 0.7° in a solar synchronous orbit at an altitude of 505 km (Figure 6). The diameter of the spot illuminated by the laser pulse is 17.5 m. The distances between two successive spots are approximate 12.25 and 2.4 km in the cross-track direction and along-track direction, respectively. The return pulse can be converted to an analog waveform based on a linear detection mode of avalanche photodiode [15]. Laser optical axis surveillance camera (LOASC) analyzes the laser pointing stability by capturing two laser beams without surface features (Tables 12 and 13).

Table 11: The specifications of the DPC sensor.

Parameter	Value	Parameter	Value
Instrument FOV	±50° (across/along-track)	Polarized angle	0°, 60°, 120°
Spatial res. (km)	>3.5	Stokes parameters	I, Q, U
Swath width (km)	1850	Rad. Cal. error	≤5%
Multiangle	≥9	Pol. Cal. error	≤0.02
Image pixels	512 × 512	Band width (nm)	20, 20, 20, 20, 10, 40, 40, 20
Spectral band (nm): P for polarization	443, 490 (P), 565, 670 (P), 763, 765, 865 (P), 910		

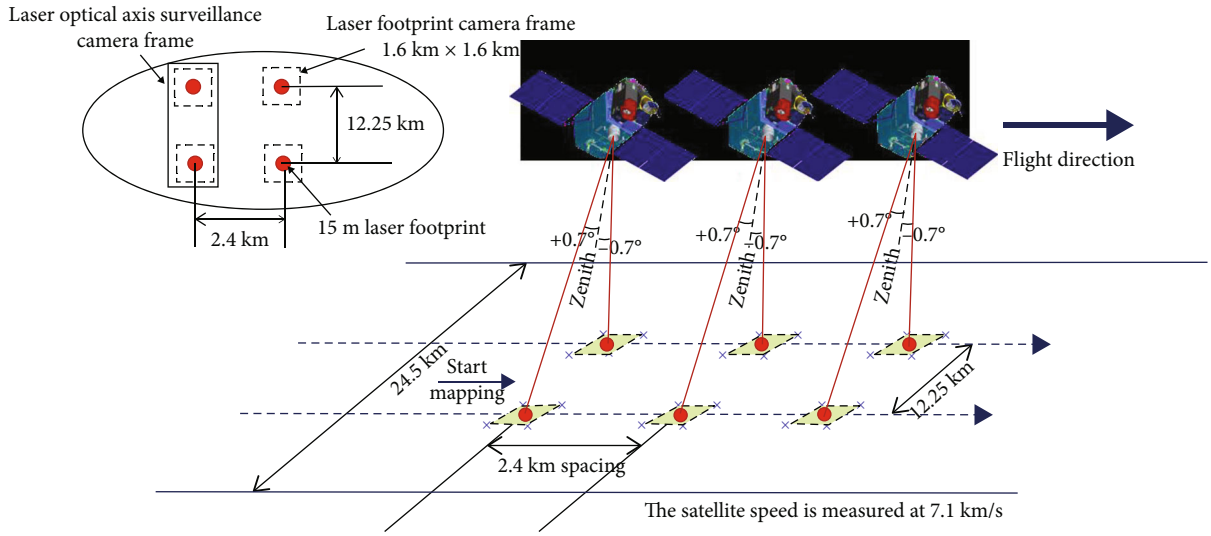

Figure 6: Schematic diagram of the GF-7 spaceborne laser altimeter system [10].

Table 12: Basic design parameters of the GF-7 laser altimeter [10].

Parameter	Value
Number of beams	2
Laser wavelength	1064 nm
Laser energy	100~180 mJ (adjustable)
Emission pulse width	4~8 ns
Laser divergence angle	30~40 μrad
Receiving telescope aperture	600 mm
Pulse repetition frequency	3/6 Hz
Echo digitization interval	0.5 ns
Laser ranging range	450~550 km
Laser ranging accuracy	≤0.3 m (slope less than 15°)

Table 13: Basic parameters of the GF-7 LFC [10].

Parameters	LFC
Spectral range	Visible light 500-700 nm Laser 1064 nm
Instantaneous field of view	6.4 μrad
Modulation Transfer Function (MTF)	≥0.20
Pixel size	16.5 μm
Image size	550 × 550 pixels
Field of view	±0.1°
Optical aperture	600 mm
Principal distance	LFC 1: 2580.2 mm LFC 2: 2576.3 mm

3. Data Application

A number of products are expected from the CHEOS, and the selected products grouped by type of sensors are presented as follows.

3.1. Forest Fire Monitoring Using GF-1/2/4/6 Images. Sensors aboard GF-1, GF-2, and GF-6 satellites can provide images with high spatial resolution and low temporal resolution. Although the staring satellite GF-4 can image at a minute-level frequency, its individual scene only covers a region of 400 × 400 km^2. Here, forest fire monitoring was taken as a case study to show the necessity of the synergy of multi-source Gaofen satellites.

At about 16:00 on May 30, 2020 (local time), a raging forest fire (102°12′7″E, 27°52′24″N) occurred in Jingjiu township in Xichan, killing 18 firefighters and a local guide and injuring three other firefighters. During the burning of

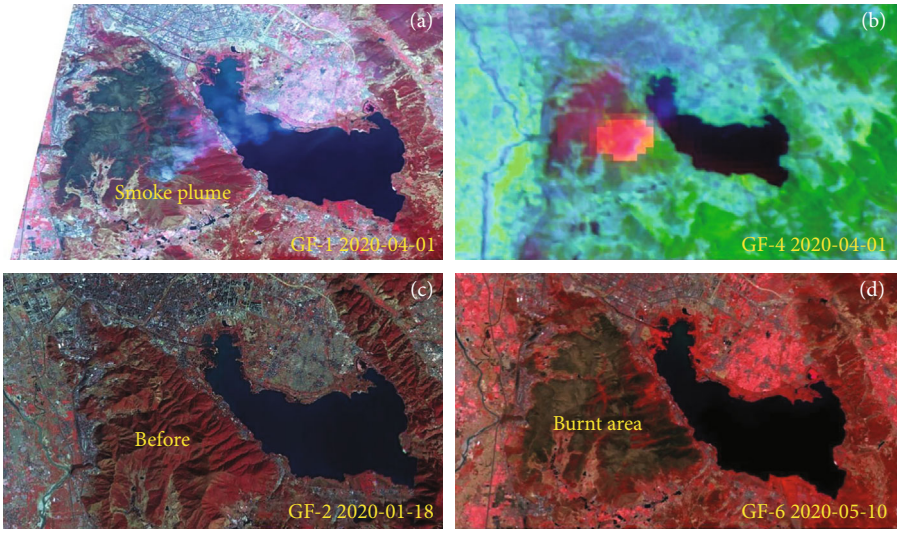

Figure 7: High-resolution satellite images during the "3·30" Xichang forest fire: (a) GF-1/PMS false color image (bands 4-3-2) at 11:57 on April 1, 2020; (b) GF-4/PMI false color image (bands 6-5-4) at 11:31 on April 1, 2020; (c) GF-2/MSS false color image (bands 5-4-3) at 11:30 on January 18, 2020; (d) GF-6/WFI false color image (bands 4-3-2) at 11:30 on May 10, 2020.

"3·30" Xichang forest fire, GF-1/PMS captured the burn scar and large smoke plume led by strong wind from space at 11:57 on April 1, 2020 (Figure 7(a)). Meanwhile, the GF-4 satellite was arranged to track the real-time spread of Xichang forest fire. The GF-4/PMI false color image (Figure 7(b)) composed of the GF-4/PMI MWIR, NIR, and R bands was characterized by active fires shown in bright red, burnt region shown in darker red, and the region covered with vegetation shown in green. With four days of fire-fighting, this wildfire was extinguished on April 2, 2020. A GF-2/MSS image on January 18, 2020 (prefire), and a GF-6/WFI image on May 10, 2020 (postfire), were obtained to access the burnt scar of Xichang forest fire. And the final burnt area covered approximately 2700 hectares.

In addition, GF-2 satellite data will set up a high-resolution integrated traffic remote sensing application demonstration system to carry out traffic network planning, traffic network monitoring, and traffic travel services in Xinjiang, Yangtze River Basin, Beijing, and other areas.

3.2. Working Principle and Image Features of GF-3. It can observe the Earth in 12 operating modes (Table 4) from single polarization to dual polarization and full polarization, with resolution of 1 to 500 meters and strip width of 5 to 650 km to meet different application requirements. GF-3 revisits the same point on Earth for up to 3.5 days. This feature makes GF-3 suitable for resource monitoring. As the subaperture images are combined, the resolution increases until the full resolution is obtained. This creates a pipeline of subaperture data streams through which the data is recorded and accumulated to gradually produce the final imaging result. With the high-precision GF-3 radar map of local areas in China, we could see the distribution map of rural villages in Zhoukou area of Henan Province, Poyang Lake of Jiangxi Province, Chongqing fold in Chongqing, and Tongling water transport ships of Anhui Province (Figure 8).

3.3. GF-5 Data Products and Applications. DPC provides cloud and aerosol properties related to the monitoring of atmospheric environments and yield of climate datasets, which is essential to the estimation of surface radiation [16]. The POLDER onboard PARASOL satellite has demonstrated the effectiveness of polarized measurements and their unique advantages in retrieving cloud properties (e.g., cloud droplet size distribution) [17, 18]. The accuracy of cloud retrieval has been also demonstrated by APS sensors developed by NASA [19]. A full retrieval suite of global cloud properties would be provided by DPC in the near future [20, 21]. It is expected that the accuracy of cloud detection, cloud phase, and cloud top pressure products should be above 85% (Figure 9).

A number of products are expected to be derived from the GF-5 satellite. For EMI, the vertical column amount of total or tropospheric NO_2, O_3, SO_2, BrO, and HCHO will be retrieved at an accuracy of better than 20%. Figure 10 depicts the global NO_2 column density means of EMI and TROPOMI in January 2019 with a correlation coefficient up to 0.93, where the low values are in the tropics, and there is a high-level pollution situation of NO_2 in North China [5]. The main mission of GMI is to provide global coverage of the column-averaged dry-air mole fraction of CO_2 and CH_4 products. The AIUS is aimed at detecting the O_3, H_2O, CO, HNO_3, NO, NO_2, N_2O, HCl, and HF profiles in the middle and upper atmosphere. The retrieved O_3, HCl, and N_2O profiles from AIUS are shown in Figure 11. By comparing with the corresponding Aura MLS and ACE-FTS level 2 products, the relative deviation of derived AIUS O_3, HCl, and N_2O profiles is less than 50%, 20%, and 20% below the height of 30 km, respectively.

3.4. GF-7 Data Applications in 3D Landscape Monitoring. GF-7 is designed to provide high-quality orthoimages and stereo images. The high-resolution stereo camera and a dual beam laser altimeter are enabled with full waveform sampling

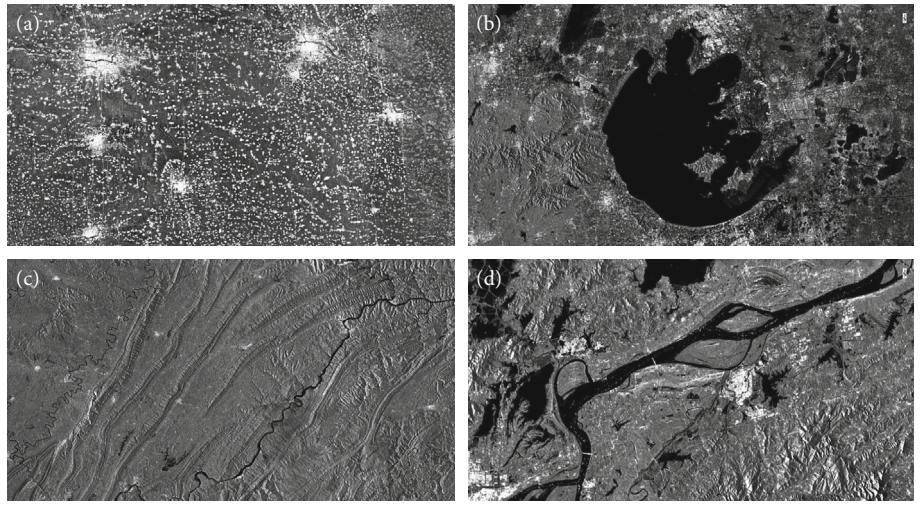

Figure 8: GF-3 radar remote sensing image map in (a) Zhoukou, Henan; (b) Poyang Lake, Jiangxi; (c) Chongqing fold, Chongqing; (d) Tongling, Anhui.

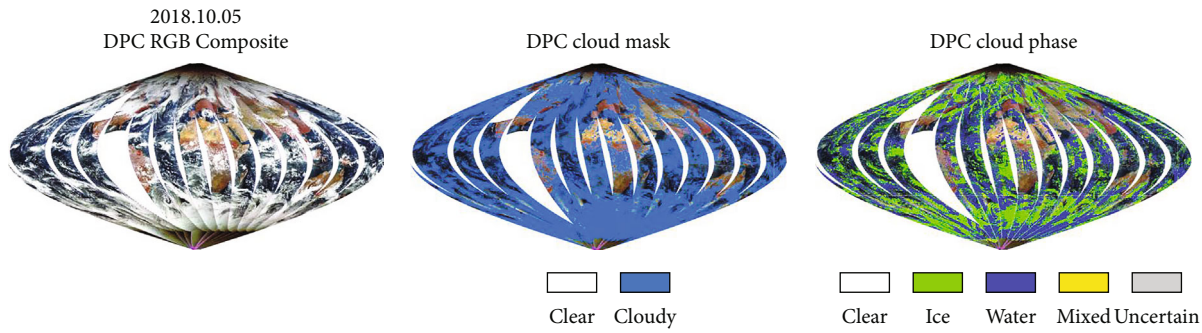

Figure 9: The true-color image, cloud mask, and cloud phase derived from DPC on 28 October 2018.

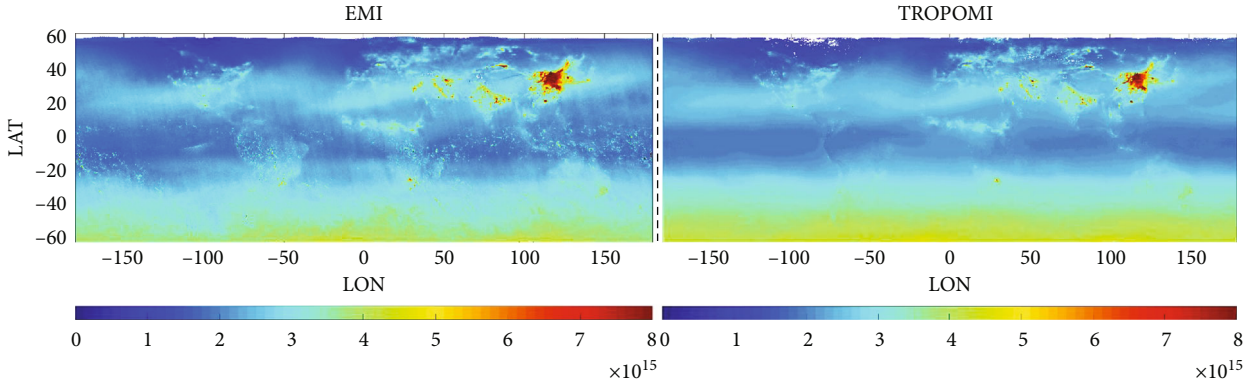

Figure 10: Monthly averaged NO_2 column density from EMI (top) and TROPOMI (bottom) in January 2019.

and recording functions. The dual-line array panchromatic camera with the spatial resolution of 0.65 m is composed of forward-looking and rear-looking cameras which can produce stereo-image pairs in the same orbit. It can reach a 1 : 10000 scale stereo-mapping accuracy by combining with laser altimeter data. The emission and echo waveforms of the GF-7 laser altimeter are sampled at intervals of 0.5 ns, and 400 and 800 sampling values are recorded at each laser point. Figure 12 presents the 3D buildings in the Fangshan District, Beijing, with GF-7 stereo data. The digital surface model produced by the three-dimensional remote sensing satellite and the three-dimensional information of the single building accurately express the topographic features and the three-dimensional landscape of the city. In the future, satellite remote sensing technology will be used to implement large-scale regular updates of urban 3D scenes and 3D building data.

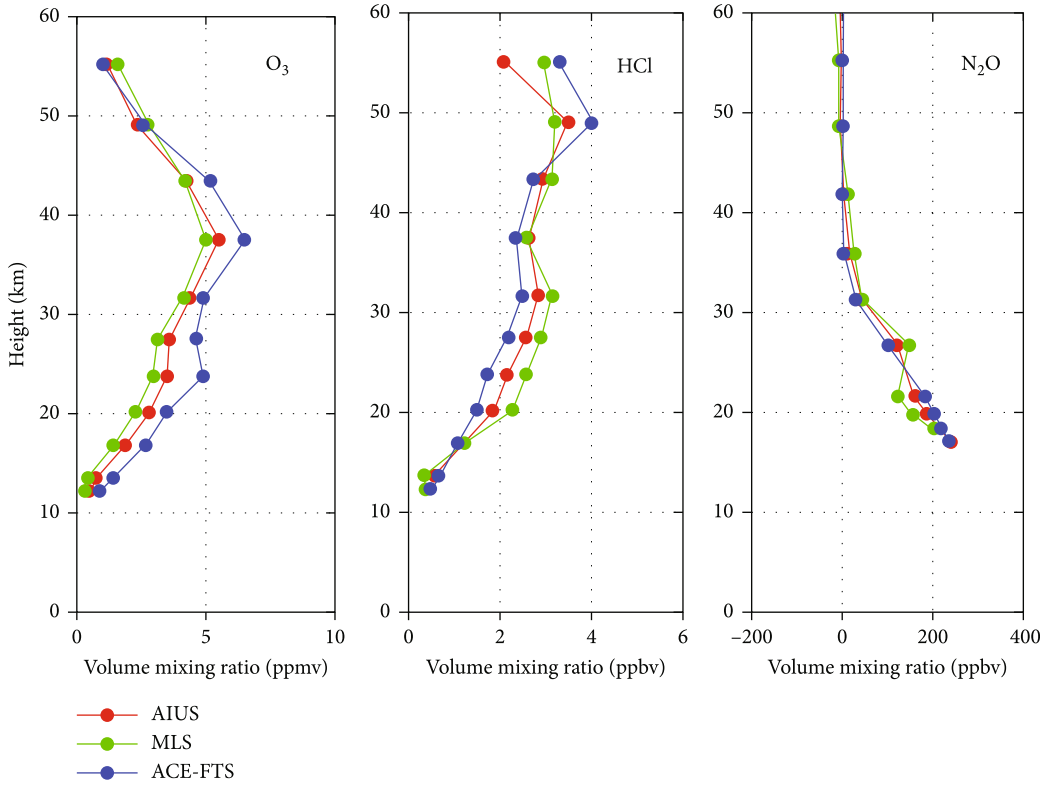

Figure 11: Retrieved profiles of O_3, HCl, and N_2O from GF-5-AIUS and the comparison with MLS and ACE-FTS products.

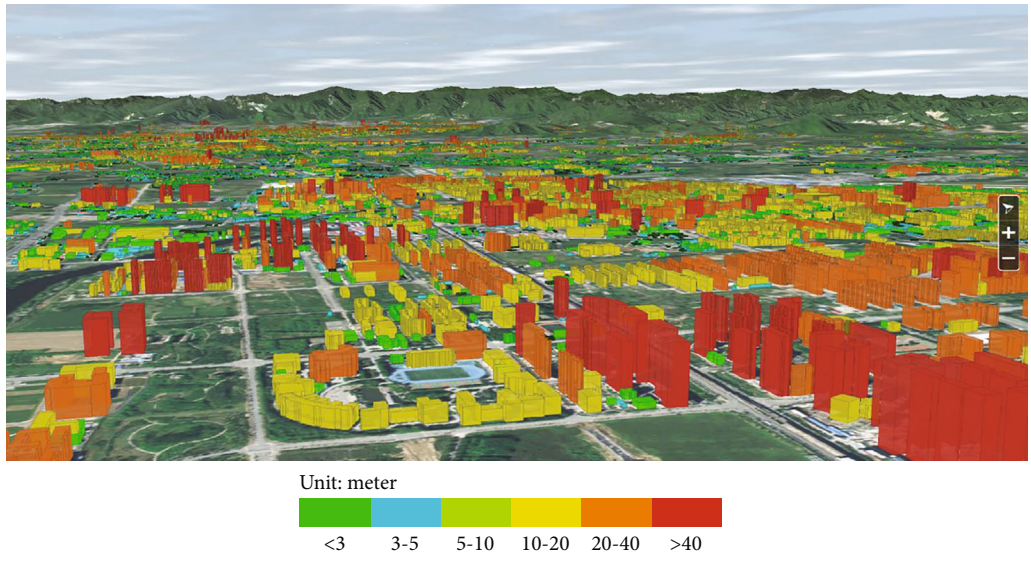

Figure 12: 3D buildings in the Fangshan District, Beijing, with GF-7 satellite data.

4. Conclusion

The CHEOS marks that China's remote sensing satellite has entered the "era of high resolution." So far, there are three high spatial resolution multispectral satellites, namely, GF-1, GF-2, and GF-6, one high-resolution radar satellite (GF-3), one optical geostationary satellite (GF-4), one hyperspectral atmospheric observation satellite (GF-5), and one three-dimensional mapping satellite (GF-7).

GF-1 has the advantages in large-scale surface observation including environmental monitoring. The GF-2 satellite system is China's highest resolution optical Earth observation satellite, and its spatial resolution is accurate to 1 meter for the first time. GF-1 can be used for a wide range of

census; GF-2 can be used for detailed survey of precise fixed points. The two satellites have their own characteristics and can be used together. The GF-6 satellite carries a 2-meter panchromatic with an 8-meter multispectral high-resolution camera and a 16-meter multispectral medium resolution broadband camera similar to GF-1. It can obtain large-scale Earth observation data through networking with the GF-1 satellite. Besides, the successive satellites like GF-1 02-04 and GF-5 02 are planned to provide densified observation.

GF-4 has been in orbit for more than four years, providing nearly 600,000 image data for various fields and making great contributions to the construction and development of various industries. It provides new technology for the early warning and prediction of accidental disasters, drought detection in large areas, regional flood disaster detection, typhoon detection and early warning, and the acquisition of tectonic information for seismic regions. The GF-5 satellite is the highest spectral resolution satellite in China, which can effectively detect atmospheric environment and global climate change. Hence, the satellite can accurately detect the distribution, variation, and transportation process of major atmospheric pollutants such as haze, ozone, nitrogen dioxide, and sulfur dioxide. For example, during the International Import Expo in China, which is held in November 2018 in Shanghai, the Environmental Trace Gases Monitoring Instrument on the GF-5 satellite was used to detect the pollution gases in the Yangtze River delta area, which provided the technical support for the air quality assurance of the Expo.

Acronyms

CHEOS:	Chinese High-resolution Earth Observation System
CNSA:	China National Space Administration
EOSDC-CNSA:	Earth Observation System and Data Center of CNSA
TROPOMI:	TROPOspheric Monitoring Instrument
GF:	Gaofen = high resolution
OMI:	Ozone Monitoring Instrument
C-SAR:	C-band multipolarization Synthetic Aperture Radar
AHSI:	Advanced Hyperspectral Imager
VIMS:	Visual and Infrared Multispectral Sensor
AIUS:	Atmospheric Infrared Ultraspectral Sensor
EMI:	Environment Monitoring Instrument
GMI:	Greenhouse gas Monitoring Instrument
DPC:	Directional Polarimetric Camera
SHS:	Spatial Heterodyne Spectroscopy
MWIR:	Medium-wave infrared
VNIR:	Visible/near infrared
NIR:	Near infrared
SWIR:	Short-wave infrared
TIR:	Thermal infrared
UV:	Ultraviolet
Vis:	Visible spectral
CCD:	Charge Coupled Device
APD:	Avalanche photodiode
LFC:	Laser Footprint Camera
LOASC:	Laser optical axis surveillance camera

Data Availability

The satellite data was obtained from the resource satellite data distribution platform (http://36.112.130.153:7777/DSSPlatform/index.html).

Conflicts of Interest

The authors declare no conflict of interest.

Authors' Contributions

Conceptualization was performed by Liangfu Chen and Husi Letu; methodology was performed by Liangfu Chen, Husi Letu, Meng Fan, and Huazhe Shang; investigation was performed by Jinhua Tao, Laixiong Wu, Ying Zhang, Chao Yu, and Jianbin Gu; writing (original draft preparation) was performed by Liangfu Chen, Husi Letu, Meng Fan, Huazhe Shang, Ning Zhang, Jin Hong, and Zhongting Wang; writing (review and editing) was performed by Husi Letu, Meng Fan, Laixiong Wu, and Tianyu Zhang. Dr. Liangfu Chen and Dr. Husi Letu concepted the study; Dr. Meng Fan and Dr. Huazhe Shang drafted the manuscript; Dr. Jinhua Tao, Mrs. Laixiong Wu, Dr. Ying Zhang, Dr. Chao Yu1, Dr. Jianbin Gu, and Dr. Ning Zhang collected satellite data and produced figures; Dr. Jin Hong, Dr. Zhongting Wang, and Dr. Tianyu Zhang edited and revised the manuscript.

Acknowledgments

We thank Dr. Tao Li for providing the GF-3 radar data. We also thank Dr. Ji Dabin for providing help in data processing. We thank the Resource Satellite Application Center for providing the data available for download. This study was supported by the National Natural Science Foundation of China (Grant Nos. 41830109, 42025504, 42175152, 41871254, and 41701406).

References

[1] X. Tong, W. Zhao, J. Xing, and W. Fu, "Status and development of China High-Resolution Earth Observation System and application," in *2016 IEEE International Geoscience and Remote Sensing Symposium (IGARSS)*, Beijing, China, 2016.

[2] X. Gu and X. Tong, "Overview of China earth observation satellite programs [space agencies]," *IEEE Geoscience and Remote Sensing Magazine*, vol. 3, no. 3, pp. 113–129, 2015.

[3] A. Yang, B. Zhong, S. Wu, and Q. Liu, "Radiometric cross-calibration of Gf-4 in multispectral bands," *Remote Sensing*, vol. 9, no. 3, p. 232, 2017.

[4] M. Zhao, F. Si, Y. Wang et al., "First year on-orbit calibration of the Chinese environmental trace gas monitoring instrument onboard GaoFen-5," *IEEE Transactions on Geoscience and Remote Sensing*, vol. 58, no. 12, pp. 8531–8540, 2020.

[5] L. Cheng, J. Tao, P. Valks et al., "No2 retrieval from the Environmental trace gases Monitoring Instrument (EMI): preliminary results and intercomparison with OMI and TROPOMI," *Remote sensing*, vol. 11, no. 24, p. 3017, 2019.

[6] C. Zhang, C. Liu, K. L. Chan et al., "First observation of tropospheric nitrogen dioxide from the Environmental Trace Gases

Monitoring Instrument onboard the GaoFen-5 satellite," *Light: Science & Applications*, vol. 9, no. 1, p. 66, 2020.

[7] H. Shi, Z. Li, H. Ye, H. Luo, W. Xiong, and X. Wang, "First level 1 product results of the Greenhouse Gas Monitoring Instrument on the Gaofen-5 satellite," *IEEE Transactions on Geoscience and Remote Sensing*, vol. 59, no. 2, pp. 899–914, 2021.

[8] X. Li, J. Xu, T. Cheng et al., "Monitoring trace gases over the Antarctic using Atmospheric Infrared Ultraspectral Sounder onboard GaoFen-5: algorithm description and first retrieval results of O_3, H_2O, and HCl," *Remote Sensing*, vol. 11, no. 17, p. 1991, 2019.

[9] X. Tang, J. Xie, R. Liu et al., "Overview of the GF-7 laser altimeter system mission," *Earth and Space Science*, vol. 7, no. 1, 2020.

[10] J. Xie, G. Huang, R. Liu et al., "Design and data processing of China's first spaceborne laser altimeter system for earth observation: GaoFen-7," *IEEE Journal of Selected Topics in Applied Earth Observations and Remote Sensing*, vol. 13, pp. 1034–1044, 2020.

[11] L. Zhang, *Research and Implementation of Ship Target Detection Algorithm in Gf-3 Sar Imaging*, Xidian University, 2018.

[12] Z. Qingjun, "System design and key technologies of the GF-3 satellite," *Acta Geodaetica et Cartographica Sinica*, vol. 46, no. 3, pp. 269–277, 2017.

[13] Y. N. Liu, D. X. Sun, X. N. Hu et al., "The Advanced Hyperspectral Imager: aboard China's GaoFen-5 satellite," *IEEE Geoscience and Remote Sensing Magazine*, vol. 7, no. 4, pp. 23–32, 2019.

[14] X. Meng, J. Cheng, and S. Zhou, "Retrieving land surface temperature from high spatial resolution thermal infrared data of Chinese Gaofen-5," in *Paper presented at the IGARSS 2019 - 2019 IEEE International Geoscience and Remote Sensing Symposium*, Yokohama, Japan, 2019.

[15] C. Ren, J. Xie, X. Zhi, Y. Yang, and S. Yang, "Laser spot center location method for Chinese spaceborne GF-7 footprint camera," *Sensors*, vol. 20, no. 8, p. 2319, 2020.

[16] H. Letu, T. Y. Nakajima, T. Wang et al., "A new benchmark for surface radiation products over the East Asia-Pacific region retrieved from the Himawari-8/AHI next-generation geostationary satellite," *Bulletin of the American Meteorological Society*, vol. 103, no. 3, pp. E873–E888, 2022.

[17] D. Tanré, F. M. Bréon, J. L. Deuzé et al., "Remote sensing of aerosols by using polarized, directional and spectral measurements within the A-TRAIN: the PARASOL mission," *Atmospheric Measurement Techniques*, vol. 4, no. 7, pp. 1383–1395, 2011.

[18] F.-M. Breon and M. Doutriaux-Boucher, "A comparison of cloud droplet radii measured from space," *IEEE Transactions on Geoscience and Remote Sensing*, vol. 43, no. 8, pp. 1796–1805, 2005.

[19] M. D. Alexandrov, D. J. Miller, C. Rajapakshe et al., "Vertical profiles of droplet size distributions derived from cloud-side observations by the research scanning polarimeter: tests on simulated data," *Atmospheric Research*, vol. 239, article 104924, 2020.

[20] H. Shang, H. Letu, L. Chen et al., "Cloud thermodynamic phase detection using a directional polarimetric camera (DPC)," *Journal of Quantitative Spectroscopy and Radiative Transfer*, vol. 253, article 107179, 2020.

[21] L. S. Wei, H. Z. Shang, L. T. Husi et al., "Cloud detection algorithm based on GF-5 DPC data," *National Remote Sensing Bulletin*, vol. 25, no. 10, pp. 2053–2066, 2021.